

See discussions, stats, and author profiles for this publication at: <https://www.researchgate.net/publication/231661923>

# Photochemistry of Nitrosyl Metalloporphyrins: Mechanisms of the Photoinduced Release and Recombination of NO

ARTICLE *in* THE JOURNAL OF PHYSICAL CHEMISTRY B · AUGUST 1998

Impact Factor: 3.3 · DOI: 10.1021/jp9811169

---

CITATIONS

22

---

READS

10

## 4 AUTHORS, INCLUDING:



**Abhay Kini**

Purdue University

6 PUBLICATIONS 366 CITATIONS

SEE PROFILE



**Bruce H Morimoto**

Celerion

35 PUBLICATIONS 655 CITATIONS

SEE PROFILE



**Clifford P. Kubiak**

University of California, San Diego

246 PUBLICATIONS 8,453 CITATIONS

SEE PROFILE

# Photochemistry of Nitrosyl Metalloporphyrins: Mechanisms of the Photoinduced Release and Recombination of NO

Igor S. Zavarine, Abhay D. Kini, Bruce H. Morimoto, and Clifford P. Kubiak\*,†

Department of Chemistry, Purdue University, 1393 Brown Laboratory, West Lafayette, Indiana 47907

Received: February 12, 1998; In Final Form: June 8, 1998

A series of substituted nitrosylmetalloporphyrins of the type  $M(\text{NO})(\text{meso-tetra}(p\text{-X})\text{phenylporphyrin})$  ( $M = \text{Co}, \text{Mn}$ ;  $X = \text{H}, \text{NO}_2, \text{OMe}$ ) were prepared and studied by laser flash photolysis. The kinetics of the recombination reactions between the metalloporphyrins and NO in THF were examined. The recombination mechanism appears to be more complicated than the simple second-order process previously reported. Out-of-plane puckering of the porphyrin ring immediately after denitrosylation is one possible explanation. Kinetic experiments and NO transfer studies between manganese and cobalt porphyrins suggest that these compounds exist in equilibrium with NO in solution. Varying the substituents in the phenyl ring of the tetraphenylporphyrin ligand has little effect on rates of recombination with NO.

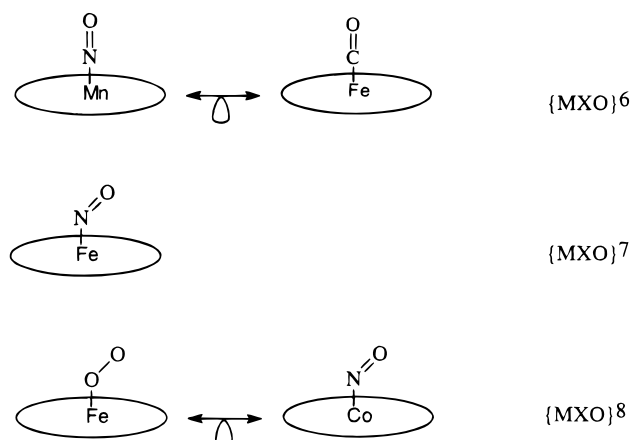
## Introduction

Nitric oxide (NO) has emerged as an important biological messenger involved in the regulation of blood pressure, as a neurotransmitter, and as a cytotoxic agent.<sup>1–7</sup> NO is also a difficult molecule to study because it rapidly oxidizes to form  $\text{NO}_2$ , and in water,  $\text{NO}_2$  subsequently dissociates into an acidic mixture of nitrite and nitrate. The reactive nature of NO has made it difficult to understand the effect NO has on its receptors. The availability of molecules that can be triggered to release NO can help in understanding the biological role of NO and could also be potentially developed as therapeutic agents.<sup>8,9</sup> Reagents that can trigger NO release in situ have been sought by several groups.

Most of the known NO donor systems rely on the formation of nitric oxide by either simple dissociation or by a complex series of reactions, often requiring metabolism in the cell.<sup>10</sup> There are only a few known cases where NO release is triggered photolytically. Of the known systems, most suffer from a number of disadvantages. For example, photolysis of  $\text{Ru}(\text{NO})\text{Cl}_3$  releases not just NO but toxic products as well.<sup>11,12</sup> Triazenes are another class of compounds tested as a NO source.<sup>11</sup> However, release of NO from these compounds requires UV light, and the quantum yields for these reactions are low (2–5%). *S*-Nitrosoglutathione releases NO under visible light, but extremely slowly.<sup>13</sup> Recently, a new system, based on *N,N'*-dimethyl-*N,N'*-dinitroso-*p*-phenylenediamine and similar compounds, was reported as a high-performance phototriggered NO source.<sup>14</sup> Although this compound was shown to be an effective NO donor, its feasibility in biological systems remains to be determined.

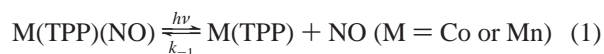
The electronic structure and geometry of the molecules described in this report can be conveniently compared in Scheme 1. Here,  $\{\text{MXO}\}^n$  represents isoelectronic homologues of small molecules, XO ( $X = \text{C}, \text{N}, \text{O}$ ), bound to metalloporphyrins of different  $d^n$  configurations.<sup>15</sup>  $\text{Mn}(\text{TPP})(\text{NO})$  is linear, isoelectronic, and isolobal to  $\text{Fe}(\text{TPP})(\text{CO})$ , while  $\text{Co}(\text{TPP})(\text{NO})$  is bent, isoelectronic, and isolobal to  $\text{Fe}(\text{O}_2)(\text{TPP})$ . This scheme

SCHEME 1



is useful for understanding the structure and reactivities of the described nitrosylmetalloporphyrins.

The photochemistry of nitrosylmetalloporphyrins has been studied in some detail.<sup>16–19</sup> M. Hoshino and co-workers have shown that NO complexes of Co(II) and Mn(II) *meso*-tetraphenylporphyrins,  $\text{Co}(\text{TPP})(\text{NO})$  (**1**), and  $\text{Mn}(\text{TPP})(\text{NO})$  (**4**) undergo efficient ( $\Phi \approx 1$ ) photodenitrosylation; see eq 1.<sup>16,17</sup>



The second-order rate constants ( $k_{-1}$ ) for the recombination reaction were reported to be  $7.0 \times 10^8 \text{ M}^{-1} \text{ s}^{-1}$  for the Co(II) complex and  $3.3 \times 10^7 \text{ M}^{-1} \text{ s}^{-1}$  for the Mn(II) complex.

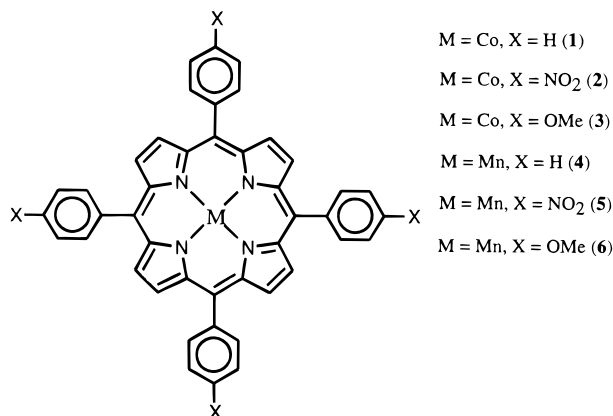
Bohle and co-workers reported a dramatic effect that different substituents on the phenyl groups of iron nitrosylmetalloporphyrins can have on NO release rates.<sup>20</sup> It was not clear whether these changes were caused by steric factors (distortion of the porphyrin core by bulky phenyl groups) or by electronic effects. The question of what effects substitution of the phenyl rings of tetraphenyl porphyrin ligands can have on the rates of the recombination reaction with NO is key in developing suitable NO release agents. Clearly, slowing the recombination rate could result in increased efficiencies of NO release.

Here we report a study of the photochemical denitrosylation and recombination mechanisms of the six different nitrosyl-

\* To whom correspondence should be addressed.

† Current Address: Department of Chemistry and Biochemistry, University of California, San Diego, 9500 Gilman Drive, Dept. 0358, La Jolla, CA 92093-0358.

metalloporphyrins: nitrosylcobalt(II) tetraphenylporphyrin (Co(TPP)(NO), **1**), nitrosylcobalt(II) *meso*-tetra(*p*-nitrophenyl)porphyrin (CoT(*p*-NO<sub>2</sub>P)P(NO), **2**), nitrosylcobalt(II) *meso*-tetra(*p*-methoxyphenyl)porphyrin CoT(*p*-OMeP)P(NO), **3**), nitrosylmanganese(II) *meso*-tetraphenylporphyrin Mn(TPP)(NO), **4**), nitrosylmanganese(II) *meso*-tetra(*p*-nitrophenyl)porphyrin MnT(*p*-NO<sub>2</sub>P)P(NO), **5**), nitrosylmanganese(II) *meso*-tetra(*p*-methoxyphenyl)porphyrin MnT(*p*-OMeP)P(NO), **6**).



## Experimental Section

**Materials.** Dichloromethane (CH<sub>2</sub>Cl<sub>2</sub>) was distilled over calcium hydride. THF was distilled from sodium benzophenone ketyl. Nitric oxide was purchased from Matheson and passed through a column of KOH pellets to remove higher oxides of nitrogen. All moisture sensitive reactions were carried out under nitrogen or argon in oven-dried glassware. All solutions for flash photolysis were prepared in a drybox using freshly distilled and dried solvents. Ultraviolet–visible spectra were obtained using a Hitachi U-2000 spectrophotometer. Infrared spectra for all compounds were obtained on a Mattson Research Series 1 spectrometer as films in dichloromethane (CH<sub>2</sub>Cl<sub>2</sub>) unless otherwise specified. Flash column chromatography was performed using silica gel 60 G 230–400 mesh (EM Science) or alumina 80–200 mesh (Fisher Scientific). The nitric oxide trap PTIO (2-phenyl-4,4,5,5-tetramethylimidazoline-1-oxyl-3-oxide) was purchased from Alexis Corp.

**Synthesis of Nitrosyl Porphyrins.** The syntheses of T(*p*-X)PPH<sub>2</sub> (X = H, OMe, NO<sub>2</sub>) were adapted from published procedures.<sup>21,22</sup> The cobalt<sup>23–25</sup> and manganese<sup>26–28</sup> metalloporphyrins were either purchased from Midcentury Chemicals or synthesized by adaptations of literature procedures.

**Synthesis of CoT(*p*-X)PP(NO) (X = H, **1**; OMe, **2**; NO<sub>2</sub>, **3**).** The nitrosylated cobalt porphyrins CoT(*p*-X)PP(NO) (X = H, **1**; OMe, **2**; NO<sub>2</sub>, **3**) were synthesized by adapting a procedure described by Scheidt and Hoard.<sup>28</sup> The cobalt porphyrins (CoT(*p*-X)PP; 200 mg) were dissolved in dichloromethane and carefully degassed. Dry piperidine (1.5 mL) was added, and NO was bubbled through a potassium hydroxide (KOH) scrubber and into the solution as a steady stream for 0.5 h. The solution was purged with nitrogen to remove excess NO and subsequently heated to boiling. The nitrosyl porphyrin precipitated after addition of degassed methanol. The products **1–3** were filtered and dried under vacuum. The yields of the nitrosylated metalloporphyrins **1–3** were ca. 50%.

**General Method for the Synthesis of Nitrosyl Derivatives of MnT(*p*-X)PP.** The nitrosylated manganese porphyrins, Mn(Cl)T(*p*-X)PP, were synthesized by adapting a procedure of Wayland and co-workers.<sup>26,29,30</sup> Mn(Cl)T(*p*-X)PP (200 mg) was added to a 100 mL round-bottom flask containing NaBH<sub>4</sub> (0.3

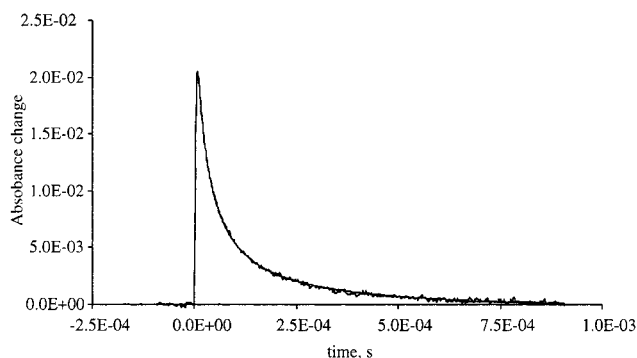


**Figure 1.** Transient observation and disappearance of the Co(TPP) species.  $\lambda_{\text{excitation}} = 532 \text{ nm}$ ;  $\lambda_{\text{observation}} = 527 \text{ nm}$ .

g). This flask was then purged with N<sub>2</sub> for 20 min. To this flask was transferred 60 mL of degassed methanol. The resulting solution was then stirred under nitrogen until evolution of hydrogen ceased completely. At this point, NO was bubbled into the solution for 20 min. Introduction of the NO results in an immediate change in the color from green to red. The nitrosylated Mn porphyrin precipitated from the solution, and this precipitate was then filtered under nitrogen. The yield of these reactions varied around 65–70%.

**Transient Absorbance Measurements.** Our basic transient absorbance instrument was described in detail previously.<sup>31</sup> Second ( $\lambda = 532 \text{ nm}$ ) or third ( $\lambda = 355 \text{ nm}$ ) harmonics of the fundamental of a Nd:YAG laser (Continuum ND60) were used for all studies, with pulse energies of 20 mJ. The excitation and the probe beam cross at a right angle. The path length was 4 mm for the excitation beam and 10 mm for the probe beam. Since the photolysis of the porphyrins leads to their slow photodecomposition, the cell was refreshed after each laser shot with a syringe pump. A second monochromator was placed between the arc lamp and the flow cell in order to minimize photolysis of the sample by the probe lamp. The transient decays were digitized (LeCroy 9400A) and transferred to a computer, and kinetics fits were performed using SigmaPlot and QuattroPro spreadsheet software.

Some transient absorbance data were obtained using a lens-intensified charge-coupled device (ICCD) as a detector. A Princeton Instruments CCD detector with a Princeton Instruments programmable pulse generator (PG-200) and an Action Research Corp. Spectra Pro-275 spectrograph were used. The 300–900 nm region of the spectrum could be observed with this instrument with the time resolution of 5 ns. With this detector, entire transient absorbance spectra were obtained at a specific delay time and then the delay time was scanned incrementally to obtain full spectra as a function of time.

**NO Concentration Determination.** The concentration of NO in the THF solutions was measured by gas chromatography (HP Series II 5890) at 27 °C. A saturated solution of NO in benzene (with a published value of NO mole fraction = 0.00109) was used for calibration.<sup>32</sup>

## Results and Discussion

**Cobalt Porphyrins.** In general, the mechanism of photodenitrosylation and NO recombination is believed to be a simple reversible process; see eq 1.<sup>16,17</sup> Our initial study focused on the kinetics of eq 1 as observed by transient UV–vis detection in the 350–630 nm region. Figure 1 shows a typical decay of photogenerated Co(TPP), monitored at 527 nm. The decay of Co(TPP) is kinetically coupled with the reformation of Co(TPP)(NO) (monitored at 540 nm), which has the same rate constant.

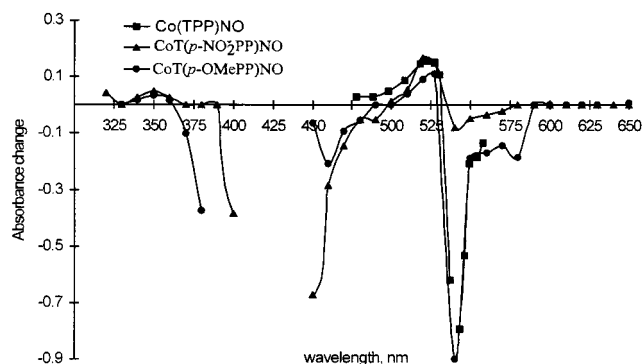


**Figure 2.** Full transient absorption spectrum of the CoTPPNO, Co-(T(*p*-NO<sub>2</sub>)PP)NO, Co(T(*p*-OMe)PP)NO system.  $\lambda_{\text{excitation}} = 532$  nm. (For Figures 2 and 6 data were not obtained in the 425 nm region due to a very intense Soret band.)

**TABLE 1: Rate Constants of the Recombination Reaction 1 in Different Solvents**

	2-MTHF <sup>16</sup>	THF (this communication)	benzene <sup>18,19</sup>
rate constant, M <sup>-1</sup> s <sup>-1</sup>	$7 \times 10^8$	$2.2 \times 10^9$	$7.9 \times 10^9$

The full transient absorption (TA) spectrum is shown in Figure 2 and it is very close to the difference of the spectra of Co-(TPP)(NO) and Co(TPP). Table 1 compares the recombination kinetics in 2-methyl-THF, THF (2-MTHF), and benzene. The NO recombination reaction is markedly solvent dependent and is found to be significantly slower in better coordinating solvents such as 2-methyl-THF and THF.

Previous studies assumed simple second-order recombination between NO radical and CoTPP.<sup>16,17</sup> We observe, however, a somewhat more complicated picture in THF. The shape of the decay curve is highly wavelength dependent, and at few selected wavelengths (527 and 540 nm, for example), decays can be fit to a second-order rate law. However at other wavelengths, the decays could not be fit to either a simple first- or second-order rate law. The behavior of the recombination reaction is even more complicated for the substituted porphyrins. For CoT(*p*-OMe)P(NO) (**3**) at  $\lambda = 510$  nm, a different reaction on a much longer time scale dominates the transient absorbance signal. For the CoT(*p*-NO<sub>2</sub>)P(NO), a complex picture emerges suggesting that at least two parallel reactions are occurring: (1) a fast process with the negative absorbance change and (2) a slower process with the positive absorbance change as observed at  $\lambda = 540$  nm; see Figure 3.

This mixed kinetics behavior could be explained by formation of a solvento species. However, the shape of the recombination curves remains similarly complex for both Co and Mn porphyrins (vide infra), and for Mn porphyrins the shape of the recombination curve is the same in benzene and THF. Therefore, competitive solvent coordination to the metal does not completely explain this complex behavior. One alternative explanation involves puckering of the porphyrin ring in solution. It has frequently been suggested that nonplanar conformations of porphyrins may play a critical role in modulating their properties in vivo. There are reports in the literature of "ruffling" of the porphyrin core and on its effects on reactivity and electronic and redox properties.<sup>33,34</sup> Axial ligands such as NO can influence the conformation of the porphyrin ring.<sup>33,34</sup> The crystal structure data of Co(TPP) at 100 K show that the molecule is essentially planar, with a deviation of the Co atom from the porphyrin plane of only 0.002 Å.<sup>35</sup> The crystal structure of the Co(TPP)(NO), however, is not planar. The Co atom is displaced from the plane of the porphyrin ligand by

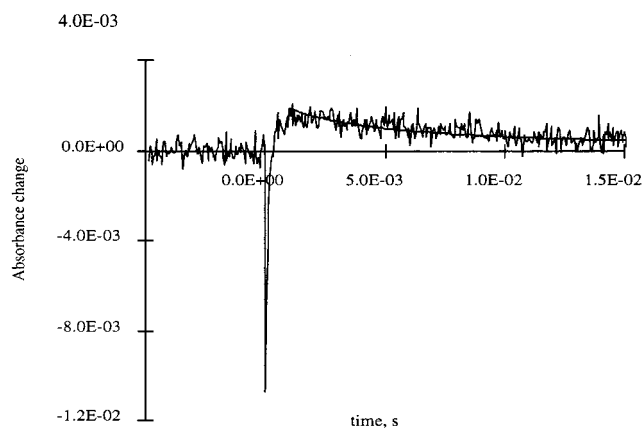
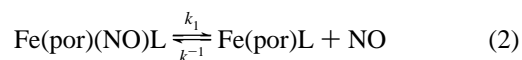


**Figure 3.** Transient formation and disappearance of "ruffled" CoT-(*p*-NO<sub>2</sub>)PP(NO) monitored at 540 nm. Solid line corresponds to the biexponential fitting of the decay.

0.094 Å, as estimated by Scheidt and Hoard, and the NO ligand is bent.<sup>28</sup> In the liquid phase, the geometries of both of these molecules are probably less rigid and a manifold of states puckered (or ruffled) to different degrees may contribute to the observed electronic spectra. Photodenitrosylation thus can change the geometry of the porphyrin from puckered (NO adduct) to planar (free metalloporphyrin). However, the available kinetic data do not preclude other processes contributing to the complex NO recombination behavior, such as M-NO geometry isomerism. The NO ligand is known to bind to metals in both linear and bent geometries.

To see the effects of porphyrin ring substituents on the rate of NO recombination, we studied the kinetics of the recombination between these substituted Co porphyrins and NO. The corresponding rates of recombination (at carefully selected wavelengths where the decay curves fit a second-order rate law) are given in Table 2. Although the effects are small, the electron-withdrawing NO<sub>2</sub> group does decrease the recombination rate, while the rate for CoT(*p*-OMe)P(NO) recombination is the same within experimental error as that for Co(TPP)(NO). The NO<sub>2</sub> group has a significantly higher Hammett's  $\sigma$  value (0.81) than does a methoxy group (-0.28), consistent with these observations.<sup>36</sup> Previously, oxidation potentials, frequencies of IR  $\nu(\text{NO})$  bands, and spectroelectrochemical behavior were found to be very similar for **1** and **3** but different from **2**.<sup>37</sup>

It is pertinent to compare our data with recent studies on the rates of ligand-induced NO dissociation from iron porphyrins.<sup>20</sup> At equilibrium, in eq 2,



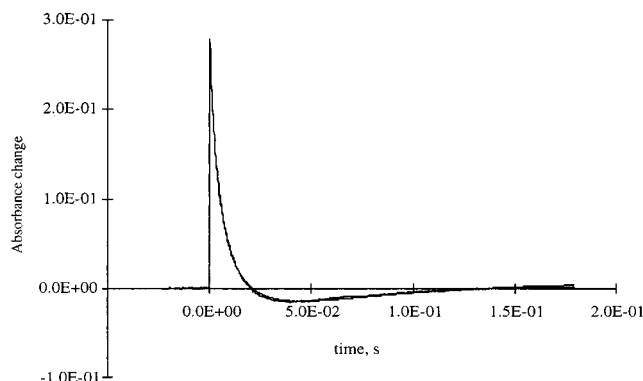
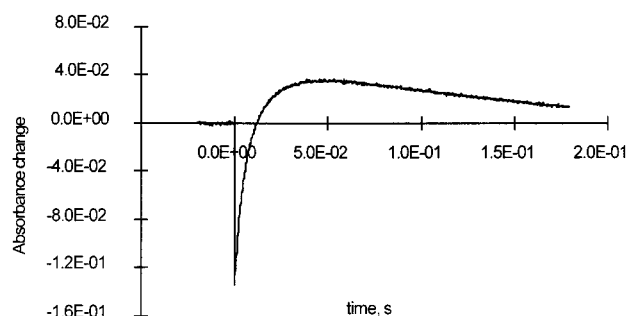
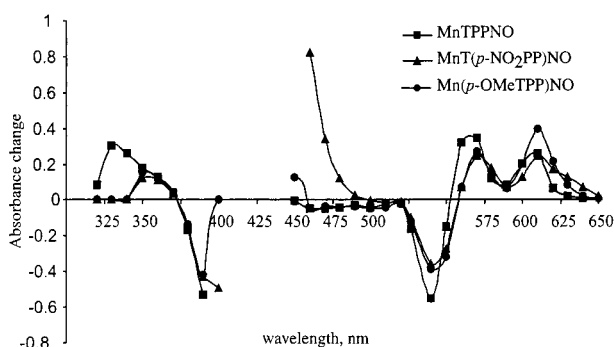
where L = pyridine or *N*-methylimidazole, a 10<sup>6</sup>-fold variation in the value of  $k_1$  in the series of tetraarylporphyrins (*p*-tolyl, 2,6-difluorophenyl, mesityl, 2,6-dichlorophenyl, and pentafluorophenyl) was reported. Our results are in sharp contrast to these observations. This could originate from the significantly distorted conformation of the porphyrins in the iron series. All of our meso para-substituted porphyrins presumably have the same (planar) conformation of the porphyrin ring and, therefore, do not significantly differ in their rates of NO recombination.

**Mn Porphyrins.** We have also investigated the NO recombination kinetics of substituted manganese nitrosyl porphyrins. Two major differences between the kinetic behavior of the Co and Mn porphyrins emerge from these studies. First, the rate of recombination between Mn porphyrins and NO is ca. 1000 times slower than those of Co porphyrins. Second, at any



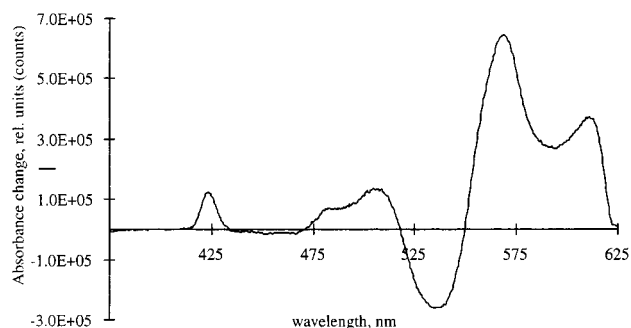
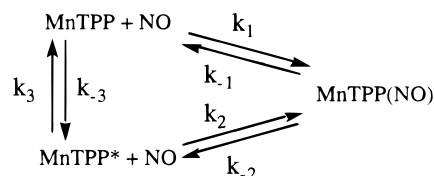
**TABLE 2: Rate Constants (in THF) of the Recombination Reaction 1 for Porphyrins with Different Substituents in the Phenyl Ring<sup>a</sup>**

	CoTPPNO (1)	CoT( <i>p</i> -OMe)PP(NO) (3)	CoT( <i>p</i> -NO <sub>2</sub> )PP(NO) (2)
rate constant, M <sup>-1</sup> s <sup>-1</sup>	2.2 × 10 <sup>9</sup>	2.3 × 10 <sup>9</sup>	1.5 × 10 <sup>9</sup>

<sup>a</sup> Estimated errors are less than 30%.**Figure 4.** Transient formation and disappearance of ruffled Mn(TPP) species;  $\lambda_{\text{excitation}} = 532$  nm.**Figure 5.** Transient photobleaching and recovery of the ruffled Mn(TPP)(NO) species;  $\lambda_{\text{excitation}} = 532$  nm.**Figure 6.** Transient absorption spectra of Mn(TPP)NO, Mn(T(*p*-NO<sub>2</sub>)PP)NO, and Mn(T(*p*-OMe)PP)NO.

wavelength, all three Mn porphyrins in this study did not exhibit the simple second-order recombination behavior previously reported. Typical decay and restoration curves show complex kinetics in both formation/decay of the Mn(TPP) species (Figure 4) and the bleaching/reappearance of Mn(TPP)(NO) (Figure 5) (though the shape of the slow components on these figures could be somewhat distorted due to the limitations of our instrument).

Full TA spectra of the compounds **4**, **5**, and **6** acquired 1 ms after the laser pulse are shown in Figure 6. Positive bands at 610, 570, and 420 nm correspond to the transient formation of the Mn(TPP) species, while the negative band at 540 nm corresponds to the photobleaching of the parent Mn(TPP)(NO) molecules. Absorptions at  $\lambda > 500$  nm involve metal d orbitals,

**Figure 7.** Full transient absorption spectrum of the Mn(TPP)(NO)/MnTPP system.**SCHEME 2**

while absorptions at  $\lambda < 500$  nm are intraligand (Soret) bands. TA spectra are virtually the same above 500 nm, except for small variations in intensities, but the bands below 500 nm are somewhat different. The bands for **4** and **5** are very similar, while the intraligand band for **6** appears to be blue-shifted by about 25 nm. It is interesting to compare the results obtained approximately 1 ms after the laser pulse with the TA spectrum (Figure 7) for **4** obtained with the ICCD detector 100 ns after the laser pulse. The regions above 500 nm are essentially identical at both times, but the intraligand absorptions for **4** below 500 nm are different at different time delays. These data are consistent with a very fast photodinitrosylation process and a relatively slow relaxation of the porphyrin ring to the non-planar equilibrium structure found in **4**.

Analysis of the kinetics supports this view. The rate of recombination between Mn porphyrins and NO is significantly slower than the corresponding rates for the Co porphyrin. The shape of the decay curve (see Figure 4 and Figure 5) indicates that at least two reactions are taking place at the same time. As with Co porphyrins, the shape of the kinetic traces varies with wavelength. At a number of wavelengths, kinetic data were simply biexponential, consistent with two parallel first-order recombination reactions. This biexponential kinetics can be explained in several ways. Perhaps, the most plausible model is a multistage equilibrium illustrated in Scheme 2, where MnTPP\* represents the puckered isomer of planar MnTPP.

The kinetic behavior of these multiequilibrium systems is well-known.<sup>38</sup> For a system with three different states, behavior is always biexponential, and for  $n$  states, there will be  $n - 1$  exponential terms.<sup>38</sup> Of course, the problem is underdetermined, and one cannot evaluate all six rate constants in Scheme 1.

One test of the model is to conduct flash photolysis of Mn(TPP)(NO) in the presence of a large and known excess of NO in the solution. Under these conditions, kinetic traces at all wavelengths become clean monoexponentials (Figure 8). This result confirms that it is a process competing with NO re-

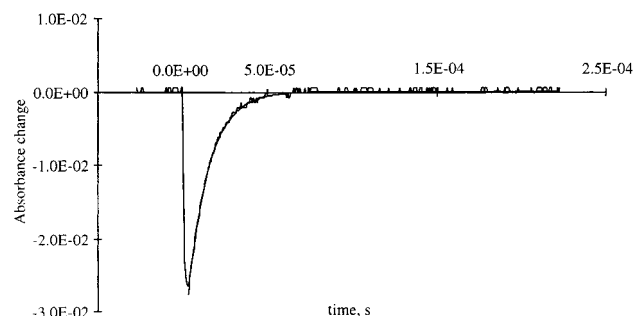


**Figure 8.** Clean pseudo-first-order photobleaching and recovery of Mn(TPP)(NO), NO in big excess.

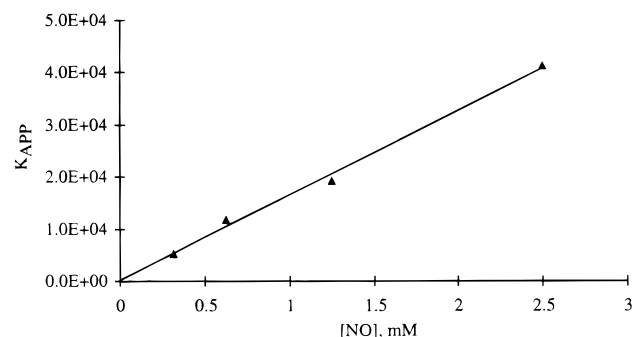


**Figure 9.** Dependence of the apparent pseudo-first-order rate constant of the Mn(TPP) recombination, with NO on the concentration of the excess NO in THF.

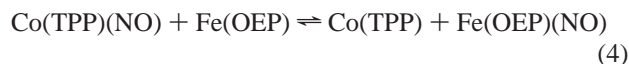
combination that causes the recombination plots to deviate from a simple second-order rate law. In the presence of the large excess of NO, the rate constants  $k_1$  and  $k_2$  from Scheme 1 become much higher than  $k_3$  as only one isomer (either MnTPP or MnTPP\*) recombines with NO. In this case, the apparent rate constant  $k_{app}$  is given by eq 3

$$k_{app} = 2k_{-n}[\text{NO}] + k_n \quad (3)$$

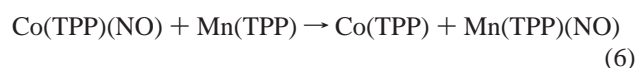
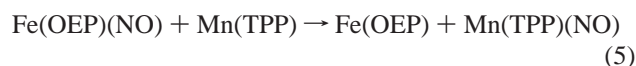
where  $n = 1$  if  $k_1 \gg k_2$  and  $n = 2$  if  $k_1 \ll k_2$ . Furthermore, the plot of  $k_{app}$  vs  $[\text{NO}]$  should be linear, with the slope being equal to  $k_{-n}$  and the intercept being equal to  $k_n$ . The plot (see Figure 9) is a straight line, but the intercept is indistinguishable from zero. Hence, the plot cannot really offer a proof of the puckering preequilibrium. The second-order recombination constant  $k_{-n}$  determined from this plot is  $1.6 \times 10^7 \text{ M}^{-1} \text{ s}^{-1}$  for Mn(TPP)(NO) (4) in THF. This value could be compared with the  $3.3 \times 10^7 \text{ M}^{-1} \text{ s}^{-1}$  value reported for this compound by Hoshino and co-workers in MTHF.<sup>16</sup> It could be argued that the observed slow reaction in our studies is simply a macrodiffusion of photoproducts from the observation region in the cell in the TA experiment. However, the magnitude of this second slower component does not change while the temperature varies from 5 to 30 °C, and we do not see this effect in flash photolysis of other systems. Both fast and slow features are present in benzene, and therefore, this slower reaction cannot realistically be attributed to the formation of a solvento species. However, the rate of the reaction is higher in benzene than it is in THF, suggesting some solvation of the Mn(TPP) species. The rate of the recombination reaction for substituted Mn porphyrins MnT(*p*-NO<sub>2</sub>P)P(NO) (5) and MnT(*p*-OMeP)P(NO) (6) follows the same trend observed for the substituted Co porphyrins: the rate constant for 5 is about 50% higher than for MnTPP(NO) (4), and the rate for 6 is essentially the same as that for 6 and 4. (Estimates only can be given for the Mn case, because the extinction coefficients for 5, 5a, 6,

and 6a are not known accurately and experimental rate constant determination requires these values.)

**NO Transfer Studies.** Kadish and co-workers showed that for the NO transfer reaction between two different metalloporphyrins

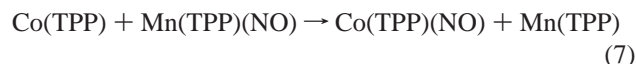


occurs on the electrochemical time scale.<sup>39</sup> They further suggest that the driving force for the NO transfer reactions is a stronger Fe–N (1.717 Å bond length) bond as compared to the Co–N bond (1.833 Å bond length). Extending these arguments to Mn porphyrins (MnTPP has even shorter bond length), they suggested and attempted (unsuccessfully) the following NO transfer reactions:



They concluded that neither the bond strength nor the linearity of the M–N–O bond is the driving force of the transfer reaction. Upon consideration of the results, described herein, that indicate that NO binds with Co porphyrins about 100 times faster than Mn porphyrins do, this result is not surprising. In fact, our kinetic study suggests that the opposite of the reaction 6 should occur.

When a 2 mM solution of the Mn(TPP)(NO) (or 5 or 6) is mixed with a 2 mM solution of Co(TPP), the NO transfer from Mn(TPP)(NO) to Co(TPP) occurs (eq 7).



This was determined by the complete disappearance of the IR  $\nu(\text{NO})$  absorption of the Mn(TPP)(NO) at  $1750 \text{ cm}^{-1}$  and the appearance of the  $\nu(\text{NO})$  band at  $1684 \text{ cm}^{-1}$ , corresponding to the Co(TPP)(NO). Hence, the nitrosyl ligand-transfer reaction from a nitrosyl cobalt porphyrin to a free manganese porphyrin could not be triggered photochemically, but it occurs readily in the dark. When Mn(TPP)(NO) is mixed with nitric oxide trap (PTIO), the band of the Mn(TPP)(NO) at  $1750 \text{ cm}^{-1}$  disappears in the IR spectrum and the Mn(TPP) stretches at 568 and 610 nm in the UV–vis spectrum appear. Hence, the thermal reactivity of Mn(TPP)(NO) together with its kinetic behavior suggests that Mn(TPP) is in equilibrium with NO in solution. In view of these results, it is not necessary to invoke the intermediacy of a bridged Mn–(NO)–Co species as suggested by Kadish and co-workers,<sup>39</sup> which would require the distance between the two big porphyrin rings in the intermediate to be unreasonably small. Existence of equilibrium between the Fe(III) porphyrins (or ferrihemoproteins) and NO in the solution was reported in the literature.<sup>40,41</sup>

## Conclusions

The mechanisms of recombination between NO and metal porphyrins are more complicated than simple second-order behavior. While Co(TPP)(NO) recombination behavior in many cases could be described as second-order recombination, Mn(TPP)(NO) recombination and reactivity suggests that Mn(TPP) exists in equilibrium with NO in solution. Kinetic evidence is presented for the formation of “ruffled” conformations of the porphyrin molecules after denitrosylation.

Photochemical NO transfer from Co(TPP)(NO) to Mn(TPP) is thermodynamically unfeasible. The NO transfer in the opposite direction, from Mn(TPP)(NO) to Co(TPP), however, occurs thermally. The relative thermodynamic stabilities of Mn(TPP)(NO) and Co(TPP)(NO) have been determined in this study, and a new mechanism for the NO transfer between two different metalloporphyrins was suggested. The effect of the substitution in the meso para position is small in comparison to substitution in other positions.

**Acknowledgment.** We acknowledge Dr. Kenneth Haber and the continued support of the Purdue Chemistry Laser Facility. This work was supported by the National Science Foundation (CHE-9319173 and CHE-9615886), by the American Heart Association, Indiana affiliate, and by funding to B.H.M. as a Cottrell Scholar of the Research Corporation.

## References and Notes

- (1) Feldman, P. L.; Griffith, O. W.; Stuehr, D. J. *Chem. Eng. News* **1993**, *71*, 26–38.
- (2) Butler, A. R.; Williams, D.; Lyn, H. *Chem. Soc. Rev.* **1993**, *4*, 233–241.
- (3) Choi, D. W. *Proc. Natl. Acad. Sci. U.S.A.* **1993**, *90*, 9741–9743.
- (4) Nathan, C. *FASEB J.* **1992**, *6*, 3051–3064.
- (5) Crossin, K. L. *Trends Biochem. Sci.* **1991**, *16*, 81–82.
- (6) Bredt, D. S.; Synder, S. H. *Neuron* **1992**, *8*, 3–11.
- (7) Moncada, S.; Palmer, R. M. J.; Higgs, E. A. *Pharmacol. Rev.* **1991**, *43*, 109–142.
- (8) Porsti, I.; Paakkari, I. *Ann. Med.* **1995**, *27*, 407–420.
- (9) Moncada, S.; Higgs, E. A. *FASEB J.* **1995**, *9*, 1319–1330.
- (10) Butler, A. R.; Glidwell, C. *Chem. Soc. Rev.* **1987**, *16*, 361–380.
- (11) Makings, L. R.; Tsien, R. Y. *J. Biol. Chem.* **1994**, *269*, 6282–6285.
- (12) Carter, T. D.; Bettache, N.; Ogden, D.; Trentham, D. R. *J. Physiol. (London)* **1993**, *467*, 165P.
- (13) Sexton, D. J.; Muruganandam, A.; MvKenney, D. J.; Mutis, B. *Photochem. Photobiol.* **1994**, *59*, 463–467.
- (14) Namiki, S.; Arai, T.; Fujimori, K. *J. Am. Chem. Soc.* **1997**, *119*, 3840–3841.
- (15) Enemark, J. H.; Feltham, R. D. *Coord. Chem. Rev.* **1974**, *13*, 339–406.
- (16) Hoshino, M.; Kogure, M. *J. Phys. Chem.* **1989**, *93*, 5478–5484.
- (17) Hoshino, M.; Arai, S.; Yamaji, M.; Hama, Y. *J. Phys. Chem.* **1986**, *90*, 2109.
- (18) Morlino, E. A.; Walker, L. A. I.; Sension, R. J.; Rogers, M. A. J. *J. Am. Chem. Soc.* **1995**, *117*, 4429–4430.
- (19) Morlino, E. A.; Rodgers, M. A. J. *J. Am. Chem. Soc.* **1996**, *118*, 11798–11804.
- (20) Bohle, S. D.; Hung, C.-H. *J. Am. Chem. Soc.* **1995**, *117*, 9584–9585.
- (21) Semeikin, A. S. K.; Berezin, B. D. *Khim. Geterotsikl. Soedin.* **1982**, *10*, 1354–1355, 1046–1047.
- (22) Bettelheim, A. W.; White, B. A.; Raybuck, S. A.; Murray, R. W. *Inorg. Chem.* **1987**, *26*, 1009–1017.
- (23) Walker, F. A.; Beroiz, D.; Kadish, K. M. *J. Am. Chem. Soc.* **1976**, *98*, 3484–3489.
- (24) Adler, A. D.; Longo, F. R.; Kampas, F.; Kim, J. *J. Inorg. Nucl. Chem.* **1970**, *32*, 2443–2445.
- (25) Buchler, J. W. *Synthesis and Properties of Metalloporphyrins*; Academic Press: New York, 1978; Vol. I, part A.
- (26) Scheidt, W. R.; Hatano, K.; Rupprecht, G. A.; Piciccolo, P. L. *Inorg. Chem.* **1978**, *17*, 292–299.
- (27) Jones, R. D.; Summerville, D. A.; Basolo, F. J. *J. Am. Chem. Soc.* **1978**, *100*, 4416–4424.
- (28) Scheidt, W. R.; Hoard, J. L. *J. Am. Chem. Soc.* **1973**, *95*, 8281–8288.
- (29) Wayland, B. B.; Olson, L. W. *Inorg. Chim. Acta* **1974**, *11*, L23–L24.
- (30) Wayland, B. B.; Olson, L. W.; Siddiqui, Z. U. *J. Am. Chem. Soc.* **1976**, *98*, 94–98.
- (31) Zavarine, I. S.; Kubiak, C. P. *Coord. Chem. Rev.* in press.
- (32) *Solubility Data Series. Oxides of Nitrogen*; Young, C. L., Ed.; Pergamon Press: Oxford, 1981; Vol. 8.
- (33) Munro, O. K.; Marques, H. M.; Debrunner, P. G.; Mohanrao, K.; Scheidt, R. W. *J. Am. Chem. Soc.* **1995**, *117*, 935–954.
- (34) Ravikanth, M.; Reddy, D.; Misra, A.; Chandrashekar, T. K. *J. Chem. Soc., Dalton Trans.* **1993**, 1137.
- (35) Stevens, E. D. *J. Am. Chem. Soc.* **1981**, *103*, 5087–95.
- (36) March, J. *Advanced Organic Chemistry*, 4th ed.; Wiley-Interscience: New York, 1992.
- (37) Kini, A. D.; Washington, J.; Kubiak, C. P.; Morimoto, B. H. *Inorg. Chem.* **1996**, *35*, 6904–6906.
- (38) Bernasconi, C. F. *Relaxation Kinetics*; Academic Press: New York, 1976.
- (39) Kadish, K. M.; Mu, X. H.; Lin, X. Q. *Inorg. Chem.* **1988**, *27*, 1489–1492.
- (40) Hoshino, M.; Ozawa, K.; Seki, H.; Ford, P. C. *J. Am. Chem. Soc.* **1993**, *115*, 9568–9575.
- (41) Laverman, L. E.; Hoshino, M.; Ford, P., C. *J. Am. Chem. Soc.* **1997**, *119*, 12663–12664.